ACTA MECHANICA SOLIDA SINICA 30 (2017) 647–657

Available online at www.sciencedirect.com

ScienceDirect

journal homepage: www.elsevier.com/locate/CAMSS

Wave propagation analysis of rotating thermoelastically-actuated nanobeams based on nonlocal strain gradient theory

*Farzad Ebrahimi**, *Parisa Haghi*

Department of Mechanical Engineering, Faculty of Engineering, Imam Khomeini International University, Qazvin, Iran

ARTICLE INFO

Article history:
Received 26 March 2017
Revised 3 September 2017
Accepted 5 September 2017
Available online 28 October 2017

Keywords:
Wave propagation
FGMS
Nonlocal strain gradient theory
Rotating nanobeam
Refined beam theory

ABSTRACT

This paper is concerned with the wave propagation behavior of rotating functionally graded (FG) temperature-dependent nanoscale beams subjected to thermal loading based on nonlocal strain gradient stress field. Uniform, linear and nonlinear temperature distributions across the thickness are investigated. Thermo-elastic properties of FG beam change gradually according to the Mori–Tanaka distribution model in the spatial coordinate. The nanobeam is modeled via a higher-order shear deformable refined beam theory which has a trigonometric shear stress function. The governing equations are derived by Hamilton's principle as a function of axial force due to centrifugal stiffening and displacement. The solution of these equations is provided employing a Galerkin-based approach which has the potential to capture various boundary conditions. By applying an analytical solution and solving an eigenvalue problem, the dispersion relations of rotating FG nanobeam are obtained. Numerical results illustrate that various parameters including temperature change, angular velocity, nonlocality parameter, wave number and gradient index have significant effects on the wave dispersion characteristics of the nanobeam under study. The outcome of this study can provide beneficial information for the next-generation research and the exact design of nano-machines including nanoscale molecular bearings, nanogears, etc.

1. Introduction

Functionally graded materials (FGMs) have been created from a mixture of ceramic and metal with a continuous variation in one or more dimensions, which are designed to reach the high structural performance. Thus, it is important to investigate the mechanical specifications of FGM structures. Recently, many papers have been published concerning the analysis of FG nanostructures. For example, the free vibration analysis of FG size-dependent nanobeam using the finite element method investigated by Eltaher et al. [1]; thermal loading effects on buckling and vibrational behavior of FG nanobeam explored by Ebrahimi et al. [2,3]; the nonlocal thermo-elastic wave propagation in temperature-dependent embedded non-homogeneous FG nanobeams presented by Ebrahimi et al. [4]; thermal environment effects on the wave dispersion behavior of inhomogeneous strain gradient FG nanobeams based on higher order refined beam theory studied by Ebrahimi and Barati [5]; the size-dependent mechanical behavior of functionally graded trigonometric shear deformable nanobeams including the neutral surface position concept studied by Ahouel et al. [6]; hydro-thermal effects on the vibration

* Corresponding author.
E-mail address: febrahimy@eng.ikiu.ac.ir (F. Ebrahimi).

https://doi.org/10.1016/j.camss.2017.09.007
0894-9166/

behavior of FG nano-beams explored by Ebrahimi and Barati [7,8]; the thermo-mechanical buckling analysis of curved functionally graded (FG) nanobeams based on the analytical solution method performed by Enrahimi and Barati [9]; and the wave propagation analysis of quasi-3D FG nanobeams in thermal environment based on nonlocal strain gradient theory conducted by Ebrahimi and Barati [10]. Then, in the rotating FG nanobeam field, Ebrahimi and Shafei [11] investigated the application of Eringen's nonlocal elasticity theory in the vibration analysis of rotating FG nano-beams.

The physical and mechanical characteristics of structures in the nanorealm, render evident size effects that make them demonstrate significant mechanical and thermal behaviors which are superior to the conventional structural materials. Therefore, nanomaterials have the potential to revolutionize critical technologies. Hence, for investigation on the mechanical behavior of nanostructures, in which the interatomic bonds possess a vital role in their regime, the classical continuum theory which disregards such a notable fact is not appropriate for this situation. Accordingly, this issue (size-effect) has been examined in the context of nonlocal continuum theories such as the nonlocal elasticity theory that was first proposed by Eringen [12,13,14]. According to this theory, the strain/stress state at any reference point is a function of the corresponding states of other points of the continuum body. Narendar and Gopalakrishnan [15] studied the small-scale influences on wave propagation of multi-walled carbon nanotubes. Wang [16] analyzed the wave propagation in fluid-conveying single-walled carbon nanotubes using the strain gradient theory. Yang et al. [17] researched wave dispersion of double-walled carbon nanotubes on the basis of size-dependent Timoshenko beam model. The wave propagation analysis of single-walled carbon nanotubes exposed to an axial magnetic field in the framework of nonlocal Euler–Bernoulli beam model was investigated by Narendar et al. [18] Aydogdu [19] studied the longitudinal wave dispersion of carbon nanotubes. Also, Filiz and Aydogdu [20] performed wave propagation analysis of functionally graded (FG) nanotubes conveying fluid embedded in elastic medium. A review on nonlocal elastic models for bending, buckling, vibration, and wave dispersion of nanoscale beams was explored by Eltaher et al. [21]

Devices in the nanometer realm with moving parts are called nano-machines. Rotating nanostructures containing molecular bearings, nanogears, nanoturbines and multiple gear systems have received notable consideration from the research community [22,23]. Hence, investigation of vibration and wave propagation of nanomachines is significant for their accurate design. Pradhan and Murmu [24] used a nonlocal beam model to investigate the flap-wise bending–vibration characteristics of a rotating nanocantilever. Narendar and Gopalakrishnan [25] explored the wave dispersion behavior of a rotating nanotube using the nonlocal elasticity theory. Aranda-Ruiz et al. [26] reported free vibration of rotating non-uniform nano-cantilevers according to Eringen's nonlocal elasticity theory. Recently, Mohammadi et al. [27] conducted vibration analysis of a rotating viscoelastic nano-beam embedded in a visco-Pasternak elastic medium and in a nonlinear thermal environment.

Moreover, the stiffness enhancement observed in the experiments and the strain gradient elasticity [28] cannot be well reproduced using Eringen's nonlocal elasticity theory. Recently, to diagnose the true effects of the two size-dependent problems on the structural responses, Lim et al. [29] reported a high-order nonlocal strain gradient theory (named the nonlocal strain gradient theory) to bring both of the size dependent scales into a single theory. The nonlocal strain gradient theory accounts the stress for both the nonlocal elastic stress field and the strain gradient stress field. It is worth mentioning that the nonlocal strain gradient theory catches the true effects of the two length scale parameters on the physical and mechanical characteristics of small-scale structures. Li et al. [30] reported vibration analysis of nonlocal strain gradient FG nano-beams. In these works, both stiffness-hardening and stiffness-softening influences on the vibration behavior of FG nanobeams were presented. It is observed that most of the studies were dedicated to buckling, statics and vibration of FG nano-beams, with only a few working in the field of wave propagation of FG small-scale beams. The flexural wave propagation in size-dependent functionally graded beams based on nonlocal strain gradient theory was investigated by Li et al. [31]. In another work, Ebrahimi and Barati [32] analyzed the flexural wave propagation of embedded S-FGM nano-beams under longitudinal magnetic field. Narendar [33] investigated the wave dispersion in functionally graded magneto-electro-elastic nonlocal rod. Recently, Ebrahimi et al. [34] reported wave propagation analysis of rotating strain gradient temperature-dependent (nonlinear distribution) FG nanobeam in thermal environment based on Euler–Bernoulli beam theory. According to the history, it is clear that the wave dispersion analysis of rotating FG thermo-elastic nanobeams based on higher-order shear deformable refined beam theory under different temperature distributions is a novel and useful topic.

This research deals with the wave dispersion characteristics of a rotating FG thermo-elastic nano-beam based on refined beam theory by using the nonlocal strain gradient theory under different temperature distributions. Material properties are supposed to change gradually across the thickness of nanobeam based on the Mori–Tanaka distribution model. The governing partial differential equations are derived by applying the Hamilton's principle in the framework of higher-order shear deformable refined beam model. An analytical solution is applied to capture required parameters. It is clear that the wave dispersion characteristics of rotating FG nanobeams are significantly affected by temperature change, angular velocity, wave number, nonlocal parameter, length scale parameter, and material graduation.

2. Theory and formulation

2.1. *Mori–Tanaka FGM nanobeam model*

The material properties of the FG nanobeam are assumed to distribute in accordance with the Mori–Tanaka model about the spatial coordinate. The Mori–Tanaka homogenization technique represents the local effective material properties including local effective bulk modules K_e and shear modules

Table 1. – Temperature-dependent coefficients for Si_3N_4 and SUS 304.

Material	Properties	P_0	P_{-1}	P_1	P_2	P_3
Si_3N_4	E(Pa)	348.43e+9	0	−3.070e−4	2.160e−7	−8.946e−11
	α(K^{-1})	5.8723e−6	0	9.095e−4	0	0
	ρ(kg/m^3)	2370	0	0	0	0
	κ(W/mK)	13.723	0	−1.032e−3	5.466e−7	−7.876e−11
	ν	0.24	0	0	0	0
SUS 304	E(Pa)	201.04e+9	0	3.079e−4	−6.534e−7	0
	α(K^{-1})	12.330e−6	0	8.086e−4	0	0
	ρ(kg/m^3)	8166	0	0	0	0
	κ(W/mK)	15.379	0	−1.264e−3	2.092e−6	−7.223e−10
	ν	0.3262	0	−2.002e−4	3.797e−7	0

μ_e in the form (Barati et al. 2016)

$$\frac{K_e - K_m}{K_c - K_m} = \frac{V_c}{1 + V_m(K_c - K_m)/(K_m + 4\mu_m/3)} \tag{1}$$

$$\frac{\mu_e - \mu_m}{\mu_c - \mu_m} = \frac{V_c}{1 + V_m(\mu_c - \mu_m)/[(\mu_m + \mu_m(9K_m + 8\mu_m)/(6(K_m + 2\mu_m))]} \tag{2}$$

where subscripts m and c define metal and ceramic, respectively, and their volume fractions are related by the following form:

$$V_c + V_m = 1 \tag{3}$$

in which the volume fractions of the ceramic and metal phases are respectively given by

$$V_c = \left(\frac{z}{h} + \frac{1}{2}\right)^p \tag{4}$$

$$V_m = 1 - \left(\frac{z}{h} + \frac{1}{2}\right)^p \tag{5}$$

Here p indicates the gradient index which determines gradual alteration of material properties through the thickness of the nanobeam. Finally, the effective Young's modulus (E), Poisson's ratio (υ) and mass density (ρ) can be expressed by:

$$E(z) = \frac{9K_e\mu_e}{3K_e + \mu_e} \tag{6}$$

$$\upsilon(z) = \frac{3K_e - 2\mu_e}{6K_e + 2\mu_e} \tag{7}$$

$$\rho(z) = \rho_c V_c + \rho_m V_m \tag{8}$$

And the thermal expansion coefficient (α) and thermal conductivity (κ) may be expressed as:

$$\frac{\alpha_e - \alpha_m}{\alpha_c - \alpha_m} = \frac{\frac{1}{K_e} - \frac{1}{K_m}}{\frac{1}{K_c} - \frac{1}{K_m}} \tag{9}$$

$$\frac{\kappa_e - \kappa_m}{\kappa_c - \kappa_m} = \frac{V_c}{1 + V_m\frac{(\kappa_c - \kappa_m)}{3\kappa_m}} \tag{10}$$

Also, the temperature-dependent coefficients of material phases can be expressed according to the following relation:

$$P = P_0(P_{-1}\,T^{-1} + 1 + P_1\,T + P_2\,T^2 + P_3\,T^3) \tag{11}$$

where, P_0,P_{-1}, P_1, P_2 and P_3 are the temperature-dependent constants which are tabulated in Table 1 for Si_3N_4 and SUS 304. The bottom and top surfaces of the FG nanobeam are fully metal (SUS 304) and fully ceramic (Si_3N_4), respectively.

2.2. *Kinematic relations*

In the framework of refined shear deformation beam theories, the displacement field of nonlocal FGM beam can be written as:

$$u_x(x, z) = u(x) - z\frac{\partial w_b}{\partial x} - f(z)\frac{\partial w_s}{\partial x} \tag{12}$$

$$u_z(x, z) = w_b(x) + w_s(x) \tag{13}$$

where, w_b , w_s indicate the components corresponding to the bending and shear transverse displacements of a point on the mid-surface of the beam, respectively; u denotes the longitudinal displacement; and $f(z)$ denotes the shape function representing the shear stress/strain distribution through the thickness of the beam. The present theory has a trigonometric function in the form (Mantari et al. 2014)

$$f(z) = z - \sin(\xi z)/\xi \tag{14}$$

where $\xi = \pi/h$. The non-zero strains of the present beam model can be expressed in the following form:

$$\varepsilon_{xx} = \frac{\partial u}{\partial x} - z\frac{\partial^2 w_b}{\partial x^2} - f(z)\frac{\partial^2 w_s}{\partial x^2} \tag{15}$$

$$\gamma_{xz} = g\frac{\partial w_s}{\partial x} \tag{16}$$

where, $g(z) = df/dz$. Also, the Hamilton's principle states that:

$$\int_0^t \delta(U + V - K)\,dt = 0 \tag{17}$$

Here, U is strain energy, V is the work done by external forces, and K is kinetic energy. The virtual strain energy can be written as:

$$\delta U = \int_v \sigma_{ij}\delta\varepsilon_{ij}\,dV = \int_v (\sigma_{xx}\delta\varepsilon_{xx} + \sigma_{xz}\delta\gamma_{xz})\,dV \tag{18}$$

Substituting Eqs. (15) and (16) into Eq. (18) yields:

$$\delta U = \int_0^L \left(N\frac{d\delta u}{dx} - M_b\frac{d^2\delta w_b}{dx^2} - M_s\frac{d^2\delta w_s}{dx^2} + Q\frac{d\delta w_s}{dx} \right) dx \tag{19}$$

in which the variables expressed in the above equation are defined as follows:

$$N = \int_A \sigma_{xx}\, dA,\ M_b = \int_A z\sigma_{xx}\, dA,\ M_s = \int_A f\sigma_{xx}\, dA,\ Q = \int_A g\sigma_{xz}\, dA \tag{20}$$

The first variation of the work done by applied forces can be expressed in the following form:

$$\delta V = \int_0^L \left(N^T \left(\frac{d(w_b + w_s)}{dx}\frac{d\delta(w_b + w_s)}{dx} \right) \right) dx \tag{21}$$

where N^T and N^R indicate the applied force due to temperature and the external force due to rotation, respectively, which can be defined by:

$$N^T = \int_{-h/2}^{h/2} E(z, T)\,\alpha(z, T)\,(T - T_0)\, dz \tag{22}$$

$$N^R = b\int_x^L \int_{-h/2}^{h/2} (\rho(z)A\Omega^2 x) dx dz \tag{23a}$$

where T_0 denotes the reference temperature and Ω denotes the angular velocity. In this research, we assume a uniform rotating FG nanobeam, with the maximum axial force considered (Narendar and Gopalakrishnan, 2011):

$$N^R_{max} = b\int_x^L \int_{-h/2}^{h/2} (\rho(z)A\Omega^2 x) dx dz \tag{23b}$$

The variation of kinetic energy can be presented by:

$$\begin{aligned}\delta K = \int_0^L \Bigg(& I_0\left[\frac{du}{dt}\frac{d\delta u}{dt} + \left(\frac{dw_b}{dt} + \frac{dw_s}{dt}\right)\left(\frac{d\delta w_b}{dt} + \frac{d\delta w_s}{dt}\right)\right] \\ & - I_1\left(\frac{du}{dt}\frac{d^2\delta w_b}{dxdt} + \frac{d^2 w_b}{dxdt}\frac{d\delta u}{dt}\right) \\ & + I_2\left(\frac{d^2 w_b}{dxdt}\frac{d^2\delta w_b}{dxdt}\right) - J_1\left(\frac{du}{dt}\frac{d^2\delta w_s}{dxdt} + \frac{d^2 w_s}{dxdt}\frac{d\delta u}{dt}\right) \\ & + K_2\left(\frac{d^2 w_s}{dxdt}\frac{d^2\delta w_s}{dxdt}\right) \\ & + J_2\left(\frac{d^2 w_b}{dxdt}\frac{d^2\delta w_s}{dxdt} + \frac{d^2 w_s}{dxdt}\frac{d^2\delta w_b}{dxdt}\right)\Bigg) dx\end{aligned} \tag{24}$$

in which

$$(I_0, I_1, J_1, I_2, J_2, K_2) = \int_A \rho(z)(1, z, f, z^2, zf, f^2) dA \tag{25}$$

The following equations are obtained by substituting Eqs. (19–23) into Eq. (17) when the coefficients of δu, δw_b and δw_s are equal to zero:

$$\frac{\partial N}{\partial x} = I_0\frac{d^2 u}{dt^2} - I_1\frac{d^3 w_b}{dxdt^2} - J_1\frac{d^3 w_s}{dxdt^2} \tag{26}$$

$$\begin{aligned}&\frac{d^2 M_b}{dx^2} + (N^T + N^R_{max})\frac{d^2(w_b + w_s)}{dx^2} \\ &= I_0\left(\frac{d^2 w_b}{dt^2} + \frac{d^2 w_s}{dt^2}\right) + I_1\frac{d^3 u}{dxdt^2} - I_2\frac{d^4 w_b}{dx^2 dt^2} - J_2\frac{d^4 w_s}{dx^2 dt^2}\end{aligned} \tag{27}$$

$$\begin{aligned}&\frac{d^2 M_s}{dx^2} + \frac{dQ}{dx} + (N^T + N^R_{max})\frac{d^2(w_b + w_s)}{dx^2} = I_0\left(\frac{d^2 w_b}{dt^2} + \frac{d^2 w_s}{dt^2}\right) \\ &+ J_1\frac{d^3 u}{dxdt^2} - J_2\frac{d^4 w_b}{dx^2 dt^2} - K_2\frac{d^4 w_s}{dx^2 dt^2}\end{aligned} \tag{28}$$

2.3. *The nonlocal FG nanobeam strain gradient model*

According to the theory of high-order nonlocal strain gradient elasticity developed by Lim et al. [29], the stress enumerates for both nonlocal elastic stress field and strain gradient stress field. Therefore, the stress can be expressed by the following relations:

$$\sigma_{ij} = \sigma^{(0)}_{ij} - \frac{d\sigma^{(1)}_{ij}}{dx} \tag{29}$$

where the classical stress $\sigma^{(0)}_{xx}$ and the higher-order stress $\sigma^{(1)}_{xx}$ are related to strain ε_{xx} and strain gradient $\varepsilon_{xx,x}$, respectively, which are defined as:

$$\sigma^{(0)}_{ij} = \int_0^L C_{ijkl}\alpha_0(x, x', e_0 a)\varepsilon'_{kl}(x')dx' \tag{30}$$

$$\sigma^{(1)}_{ij} = l^2\int_0^L C_{ijkl}\alpha_1(x, x', e_1 a)\varepsilon'_{kl,x}(x')dx' \tag{31}$$

in which, L is length of the beam, $\mathbf{C}_{ijkl}$ is the elastic constants, $e_0\,a$ and $e_1\,a$ are nonlocal parameters with the effect of nonlocal stress field taken into account, l is the material characteristic parameter (length scale parameter) that represents the influence of higher-order strain gradient field ($l = 0$gives the relation of nonlocal continuum theory). The nonlocal parameters $e_0\,a$ and $e_1\,a$ in the nonlocal functions $\alpha_0(x,x', e_0a)$ and $\alpha_1(x,x', e_1a)$ may be determined by matching the wave dispersion relation from experimental data or atomic lattice dynamics. Also, it is found that $\alpha_1(x,x', e_1a)$ and l do not present in Eringen's nonlocal elasticity theory [29]. The constitutive relation for a FGM nanobeam can be stated as:

$$\begin{aligned}&[1 - (e_1 a)^2\nabla^2][1 - (e_0 a)^2\nabla^2]\sigma_{ij} \\ &= C_{ijkl}[1 - (e_1 a)^2\nabla^2]\varepsilon_{kl} - C_{ijkl}\,l^2[1 - (e_0 a)^2\nabla^2]\nabla^2\varepsilon_{kl}\end{aligned} \tag{32}$$

It contains three length scale parameters: two of them represent the nonlocal size-effect (one of them for the lower-order nonlocal stress and the other the higher-order nonlocal stress), and the third one accounts for the size-effect induced by higher-order deformation or strain gradients. In Eq. (32), ∇^2 denotes the Laplace operator. According to the assumption in Lim et al. [29], $e_1 = e_0 = e$. By discarding terms of order $O(\nabla^2)$, the general constitutive relation in Eq. (34) can be stated as:

$$[1 - (ea)^2\nabla^2]\,\sigma_{ij} = C_{ijkl}\,[1 - l^2\nabla^2]\varepsilon_{kl} \tag{33}$$

Thus, the constitutive relations for a nonlocal refined shear deformable FG nanobeam can be expressed as:

$$\sigma_{xx} - \mu\frac{\partial^2\sigma_{xx}}{\partial x^2} = E(z)\left(\varepsilon_{xx} - \lambda^2\frac{\partial^2\varepsilon_{xx}}{\partial x^2}\right) \tag{34}$$

$$\sigma_{xz} - \mu\frac{\partial^2\sigma_{xz}}{\partial x^2} = G(z)\left(\gamma_{xz} - \lambda^2\frac{\partial^2\gamma_{xz}}{\partial x^2}\right) \tag{35}$$

where $\mu = ea^2$ and $\lambda = l$. Integrating Eqs. (34) and (35) over the cross-sectional area of the nanobeam provides the following nonlocal relations for FGM beam model as:

$$N - \mu\frac{\partial^2 N}{\partial x^2} = \left(1 - \lambda^2\frac{\partial^2}{\partial x^2}\right)\left(A\frac{\partial u}{\partial x} - B\frac{\partial^2 w_b}{\partial x^2} - B_s\frac{\partial^2 w_s}{\partial x^2}\right) - N_x^T \tag{36}$$

$$M_b - \mu\frac{\partial^2 M_b}{\partial x^2} = \left(1 - \lambda^2\frac{\partial^2}{\partial x^2}\right)\left(B\frac{\partial u}{\partial x} - D\frac{\partial^2 w_b}{\partial x^2} - D_s\frac{\partial^2 w_s}{\partial x^2}\right) - M_b^T \tag{37}$$

$$M_s - \mu\frac{\partial^2 M_s}{\partial x^2} = \left(1 - \lambda^2\frac{\partial^2}{\partial x^2}\right)\left(B_s\frac{\partial u}{\partial x} - D_s\frac{\partial^2 w_b}{\partial x^2} - H_s\frac{\partial^2 w_s}{\partial x^2}\right) - M_s^T \tag{38}$$

$$Q - \mu\frac{\partial^2 Q}{\partial x^2} = \left(1 - \lambda^2\frac{\partial^2}{\partial x^2}\right)\left(A_s\frac{\partial w_s}{\partial x}\right) \tag{39}$$

where the cross-sectional rigidities are explained as:

$$(A, B, B_s, D, D_s, H_s) = \int_A E(z)\,(1, z, f, z^2, zf, f^2)\,dA \tag{40}$$

$$A_s = \int_A g^2 G(z) dA \tag{41}$$

The governing equations of refined shear deformable FGM nanobeams in terms of displacements are obtained by substituting the N, M_b, M_s and Q of Eqs. (36)–(39), respectively, into Eqs. (26)–(28) as follows:

$$\begin{aligned}
&A\left(1 - \lambda^2\frac{\partial^2}{\partial x^2}\right)\left(\frac{\partial^2 u}{\partial x^2}\right) - B\left(1 - \lambda^2\frac{\partial^2}{\partial x^2}\right)\left(\frac{\partial^3 w_b}{\partial x^3}\right)\\
&-B_s\left(1 - \lambda^2\frac{\partial^2}{\partial x^2}\right)\left(\frac{\partial^3 w_s}{\partial x^3}\right) - I_0\frac{\partial^2 u}{\partial t^2} + I_1\frac{\partial^3 w_b}{\partial x\partial t^2} + J_1\frac{\partial^3 w_s}{\partial x\partial t^2}\\
&+\mu\left(I_0\frac{\partial^4 u}{\partial x^2\partial t^2} - I_1\frac{\partial^5 w_b}{\partial x^3\partial t^2} - J_1\frac{\partial^5 w_s}{\partial x^3\partial t^2}\right) = 0
\end{aligned} \tag{42}$$

$$\begin{aligned}
&B\left(1 - \lambda^2\frac{\partial^2}{\partial x^2}\right)\left(\frac{\partial^3 u}{\partial x^3}\right) - D\left(1 - \lambda^2\frac{\partial^2}{\partial x^2}\right)\left(\frac{\partial^4 w_b}{\partial x^4}\right)\\
&-D_s\left(1 - \lambda^2\frac{\partial^2}{\partial x^2}\right)\left(\frac{\partial^4 w_s}{\partial x^4}\right) - (N^T + N^R)\frac{\partial^2(w_b + w_s)}{\partial x^2}\\
&-I_0\left(\frac{\partial^2 w_b}{\partial t^2} + \frac{\partial^2 w_s}{\partial t^2}\right) - I_1\frac{\partial^3 u}{\partial x\partial t^2} + I_2\frac{\partial^4 w_b}{\partial x^2\partial t^2} + J_2\frac{\partial^4 w_s}{\partial x^2\partial t^2}\\
&+\mu\left((N^T + N^R)\frac{\partial^4(w_b + w_s)}{\partial x^4} + I_0\left(\frac{\partial^4 w_b}{\partial x^2\partial t^2} + \frac{\partial^4 w_s}{\partial x^2\partial t^2}\right)\right.\\
&\left.+I_1\frac{\partial^5 u}{\partial x^3\partial t^2} - I_2\frac{\partial^6 w_b}{\partial x^4\partial t^2} - J_2\frac{\partial^6 w_s}{\partial x^4\partial t^2}\right) = 0
\end{aligned} \tag{43}$$

$$\begin{aligned}
&B_s\left(1 - \lambda^2\frac{\partial^2}{\partial x^2}\right)\left(\frac{\partial^3 u}{\partial x^3}\right) - D_s\left(1 - \lambda^2\frac{\partial^2}{\partial x^2}\right)\left(\frac{\partial^4 w_b}{\partial x^4}\right)\\
&-H_s\left(1 - \lambda^2\frac{\partial^2}{\partial x^2}\right)\left(\frac{\partial^4 w_s}{\partial x^4}\right) + A_s\left(1 - \lambda^2\frac{\partial^2}{\partial x^2}\right)\left(\frac{\partial^2 w_s}{\partial x^2}\right)\\
&-(N^T + N^R)\frac{\partial^2(w_b + w_s)}{\partial x^2} - I_0\left(\frac{\partial^2 w_b}{\partial t^2} + \frac{\partial^2 w_s}{\partial t^2}\right)\\
&-J_1\frac{\partial^3 u}{\partial x\partial t^2} + J_2\frac{\partial^4 w_b}{\partial x^2\partial t^2} + K_2\frac{\partial^4 w_s}{\partial x^2\partial t^2}\\
&+\mu((N^T + N^R)\frac{\partial^4(w_b + w_s)}{\partial x^4} + I_0\left(\frac{\partial^4 w_b}{\partial x^2\partial t^2} + \frac{\partial^4 w_s}{\partial x^2\partial t^2}\right)\\
&+J_1\frac{\partial^5 u}{\partial x^3\partial t^2} - J_2\frac{\partial^6 w_b}{\partial x^4\partial t^2} - K_2\frac{\partial^6 w_s}{\partial x^4\partial t^2}) = 0
\end{aligned} \tag{44}$$

3. Solution procedures

The solution of governing equations of nonlocal thermoelastic FGM nanobeam can be presented by:

$$u(x,t) = U_n \exp[i(\beta x - \omega t)] \tag{45}$$

$$w_b(x,t) = W_{bn} \exp[i(\beta x - \omega t)] \tag{46}$$

$$w_s(x,t) = W_{sn} \exp[i(\beta x - \omega t)] \tag{47}$$

where (U_n,W_{bn},W_{sn}) are the wave amplitudes; β and ω indicate the wave number and circular frequency, respectively. Substituting Eqs. (45)–(47) into Eqs. (42)–(44) gives:

$$\left\{\begin{pmatrix} k_{11} & k_{12} & k_{13}\\ k_{21} & k_{22} & k_{23}\\ k_{31} & k_{32} & k_{33}\end{pmatrix} - \omega^2\begin{pmatrix} m_{11} & m_{12} & m_{13}\\ m_{21} & m_{22} & m_{23}\\ m_{31} & m_{32} & m_{33}\end{pmatrix}\right\}\begin{Bmatrix} U_n\\ W_{bn}\\ W_{sn}\end{Bmatrix} = 0 \tag{48}$$

where,

$$\begin{aligned}
&k_{11} = -A\beta^2(1 + \lambda^2\beta^2), \quad k_{21} = -Bi\beta^3(1 + \lambda^2\beta^2), \quad k_{12} = -k_{21}\\
&k_{22} = -D\beta^4(1 + \lambda^2\beta^2) + (N^R_{max} + N^T)\beta^2(1 + \mu\beta^2),\\
&k_{31} = -B_s i\beta^2(1 + \lambda^2\beta^2), \quad k_{13} = -k_{31}\\
&k_{32} = -D_s\beta^4(1 + \lambda^2\beta^2) + (N^R_{max} + N^T)\beta^2(1 + \mu\beta^2),\\
&k_{23} = -D_s\beta^4(1 + \lambda^2\beta^2) + (N^R_{max} + N^T)\beta^2(1 + \mu\beta^2)\\
&k_{33} = -(H_s\beta^4 + A_s\beta^2)(1 + \lambda^2\beta^2) + (N^R_{max} + N^T)\beta^2(1 + \mu\beta^2),\\
&m_{11} = -I_0(1 + \mu\beta^2)\\
&m_{21} = -I_1 i\beta(1 + \mu\beta^2), \quad m_{12} = -m_{21}, \quad m_{31} = -iJ_1\beta(1 + \mu\beta^2),\\
&m_{13} = -m_{31}, \quad m_{22} = -(I_0 + I_2\beta^2)(1 + \mu\beta^2)\\
&m_{32} = -(I_0 + J_2\beta^2)(1 + \mu\beta^2), \quad m_{23} = -(I_0 + J_2\beta^2)(1 + \mu\beta^2),\\
&m_{33} = -(I_0 + k_2\beta^2)(1 + \mu\beta^2)
\end{aligned}$$

By setting the determinant of the above matrix to zero, the circular frequency ω can be obtained. Hence, the roots of Eq. (43) can be written as:

$$\omega_1 = M_0(\beta), \omega_2 = M_1(\beta), \omega_3 = M_2(\beta) \tag{49}$$

These roots correspond to wave modes M_0, M_1 and M_2, respectively. Wave modes M_0 and M_2 are related to the flexural

Table 2. – Comparison of the wave frequency for rotating FG nanobeam. (NLTR, $\mu = 1$ nm, $\Delta T = 800$, $l = 1.5$).

β	Ω	$P=0$ Li et al.[31].	Present	$P=.2$ Li et al. [31].	Present	$P=1$ Li et al. [31].	Present	$P=5$ Li et al. [31].	Present
0.1	0	0.164617	0.106587	0.109812	0.0811336	0.0694308	0.0555902	0.058270	0.0405788
	1	0.164782	0.108673	0.109942	0.083689	0.0695951	0.0592566	0.0584509	0.0458823
	2	0.165275	0.114688	0.110329	0.0907568	0.070079	0.0674888	0.0589657	0.0578131
5	0	12.842553	12.8253	8.322701	8.16948	5.234263	5.231979	4.382287	4.359028
	1	12.842555	12.8255	8.322702	8.16952	5.234265	5.231980	4.382289	4.359033
	2	12.842562	12.8261	8.322707	8.16964	5.234271	5.231981	4.382296	4.359046
15	0	38.8989264	38.8931	25.208407	24.7478	15.853894	15.8469	13.273356	13.202798
	1	38.8989272	38.8932	25.208408	24.7478	15.853894	15.8469	13.273357	13.202800
	2	38.8989296	38.8934	25.208409	24.7479	15.853896	15.8469	13.273359	13.202804

waves, and mode M_1 is related to the extensional waves. Also, the phase velocity of waves can be calculated by the following relation:

$$c_{p(i)} = \frac{M_i(\beta)}{\beta}, i = 1, 2, 3 \tag{50}$$

which displays the dispersion relation between phase velocity c_p and wave number β for the FGM nanobeam. Also, the escape frequencies of the FG nanobeam can be obtained by setting$\beta \to \infty$. It should be noted that after the escape frequency is reached, the flexural waves will not propagate anymore.

4. Different types of thermal loading

4.1. *Uniform temperature rise (UTR)*

Temperature of the FG nanobeam is uniformly increased from the reference temperature T_0 to the final temperature T, with $\Delta T = T - T_0$.

4.2. *Linear temperature rise (LTR)*

In this state, the temperature varies linearly through the thickness of the nanobeam as follows

$$T = T_m + \Delta T(\frac{z}{h} + \frac{1}{2}) \tag{51}$$

where $\Delta T = T_c - T_m$, in which T_c and T_m are the temperature of bottom and top surfaces of the nanobeam, respectively.

4.3. *Nonlinear temperature rise (NLTR)*

In this case, the temperature varies nonlinearly through the thickness. The temperature distribution can be obtained by solving the steady-state heat conduction equation across the thickness, with the boundary conditions on the bottom and top surfaces of the nanobeam:

$$-\frac{d}{dz}\left(\kappa(z,\ T)\frac{dT}{dz}\right) = 0 \tag{52}$$

For every kind of temperature rise, the boundary conditions are considered as follows:

$$T\left(\frac{h}{2}\right) = T_c, \quad T\left(-\frac{h}{2}\right) = T_m \tag{53}$$

The solution of Eqs. (12) and (13) is:

$$T = T_m + (T_c - T_m)\frac{\int_{-\frac{h}{2}}^{z} \frac{1}{\kappa(z,T)}dz}{\int_{-\frac{h}{2}}^{\frac{h}{2}} \frac{1}{\kappa(z,T)}dz} \tag{54}$$

where $\Delta T = T_c - T_m$ indicates the temperature change.

5. Numerical results and discussions

This section is assigned to investigate the propagation characteristics of the mentioned nanobeam. This nanoscale beam is modeled based on the higher order shear deformable refined beam theory. The thickness of the nanobeam is considered to be $h = 100$ nm. The material properties of the mentioned nanobeam are reported in Table 1. The wave frequencies of the mentioned nanobeam are verified with those of Li et al. [31] for various wave numbers and angular velocities, a good agreement is observed, as reported in Table 2.

Tables 3 and 4 report the influence of angular velocity ($\Omega = 1$,3 and 5), length scale parameter, temperature change and material composition ($p = .2$, 1 and 5) on the phase velocity (c_p) of rotating refined FG nanobeam for various temperature distributions (UTR, LTR, NLTR) at $L/h = 20$.

In Table 3, it is found that, increasing angular velocity leads the increase in phase velocity for all three tables. Also, in a constant angular velocity, gradient index and temperature distribution type, the phase velocity increases due to an increase in ΔT. Furthermore, with the increase in gradient index, the phase velocity increases too. Finally, it can be seen that, for a constant value of Ω, gradient index and ΔT phase velocity decrease due to a change in the type of temperature distribution (UTR/LTR/NLTR), and vice versa for $\Delta T = 0$.

It is observed in Table 4 that, for a specific temperature distribution, phase velocity increases due to the increases in angular velocity and length scale parameter. However, with the increase in gradient index, the phase velocity decreases. In addition, for a constant value of Ω, both the gradient index and

Table 3. – Variation of phase velocity of FG nanobeam for various gradient indices, angular velocities, temperature changes and thermal loadings. ($L/h=20$, $\mu=1$ nm, $\beta=0.08$ (1/nm), $l=1$ nm).

	$P=.2$			$P=1$			$P=5$		
	$\Omega=1$	$\Omega=3$	$\Omega=5$	$\Omega=1$	$\Omega=3$	$\Omega=5$	$\Omega=1$	$\Omega=3$	$\Omega=5$
UTR									
$\Delta T=0$	5.61695	6.70877	7.976	4.25386	5.47553	5.79173	3.48769	4.97612	5.10986
$\Delta T=200$	5.5248	6.62856	7.85451	4.18573	5.39787	5.67595	3.43427	4.89626	5.00331
$\Delta T=500$	5.3587	6.47548	7.57756	3.98648	5.10782	5.27783	3.22105	4.53325	4.57983
$\Delta T=800$	5.08321	6.2028	7.05056	3.59779	4.42377	4.49009	2.80093	3.72275	3.73479
LTR									
$\Delta T=0$	5.61726	6.709	7.97607	4.25414	5.47565	5.79173	3.48798	4.97619	5.10986
$\Delta T=200$	5.51818	6.62351	7.85319	4.17951	5.39554	5.67587	3.42816	4.89508	5.0033
$\Delta T=500$	5.33957	6.46137	7.57473	3.96935	5.10389	5.27768	3.20446	4.53218	4.5798
$\Delta T=800$	5.05115	6.18121	7.0478	3.57258	4.42196	4.48998	2.77723	3.72252	3.73478
NLTR									
$\Delta T=0$	5.61726	6.709	7.97607	4.25414	5.47565	5.79173	3.48798	4.97619	5.10986
$\Delta T=200$	5.51798	6.62335	7.85314	4.17911	5.39539	5.67587	3.42786	4.89503	5.0033
$\Delta T=500$	5.33832	6.46045	7.57455	3.96707	5.10336	5.27766	3.20277	4.53206	4.5798
$\Delta T=800$	5.04794	6.17905	7.04752	3.56749	4.42159	4.48996	2.77358	3.72248	3.73478

Table 4. – Variation of phase velocity of FG nanobeam for various gradient indices, angular velocities, length scale parameters and thermal loadings. ($L/h=20$, $\mu=1$ nm, $\beta=0.08$ (1/nm), $\Delta T=800$).

	$P=.2$			$P=1$			$P=5$		
	$\Omega=1$	$\Omega=3$	$\Omega=5$	$\Omega=1$	$\Omega=3$	$\Omega=5$	$\Omega=1$	$\Omega=3$	$\Omega=5$
UTR									
$\lambda=0$	5.0685	6.18976	7.03039	3.58813	4.41063	4.47595	2.79443	3.71107	3.72293
$\lambda=1$	5.08321	6.2028	7.05056	3.59779	4.42377	4.49009	2.80093	3.72275	3.73479
$\lambda=2$	5.12707	6.24163	7.11042	3.62659	4.46284	4.53223	2.82036	3.75752	3.77017
LTR									
$\lambda=0$	5.03635	6.16819	7.02768	3.56287	4.40885	4.47585	2.77067	3.71085	3.72292
$\lambda=1$	5.05115	6.18121	7.0478	3.57258	4.42196	4.48998	2.77723	3.72252	3.73478
$\lambda=2$	5.09528	6.22001	7.10751	3.60156	4.46094	4.53211	2.79682	3.75728	3.77015
NLTR									
$\lambda=0$	5.03314	6.16603	7.02741	3.55777	4.40849	4.47582	2.76701	3.71081	3.72291
$\lambda=1$	5.04794	6.17905	7.04752	3.56749	4.42159	4.48996	2.77358	3.72248	3.73478
$\lambda=2$	5.0921	6.21784	7.10722	3.5965	4.46055	4.53209	2.79319	3.75724	3.77015

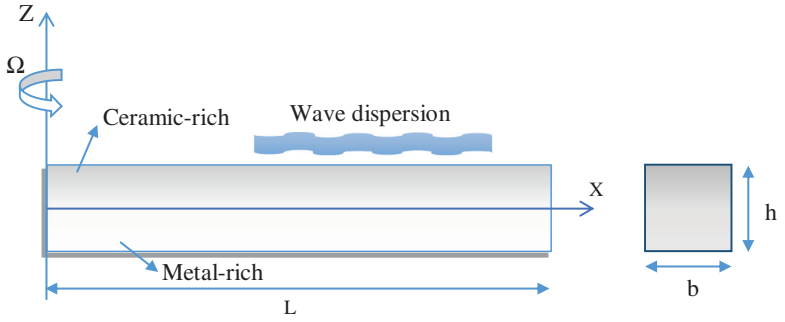

Fig. 1 – Configuration of rotating FG nanobeam.

ΔT phase velocity increase with the change in the type of temperature distribution (UTR/LTR/NLTR). (Fig. 1).

In Fig. 2. variation of the phase velocity (c_p) of rotating FG nanobeam versus wave number (β) for various angular velocities (Ω) and different values of gradient index for a constant value of nonlocality parameter ($\mu=1$ nm), length scale parameter ($\lambda=0.5$ nm) and temperature ($\Delta T=800$) for nonlinear temperature distribution model is plotted. It is observed that, in the lower values of wave number with an increase in wave number, the phase velocity increases (it is not true when $\Omega=3$

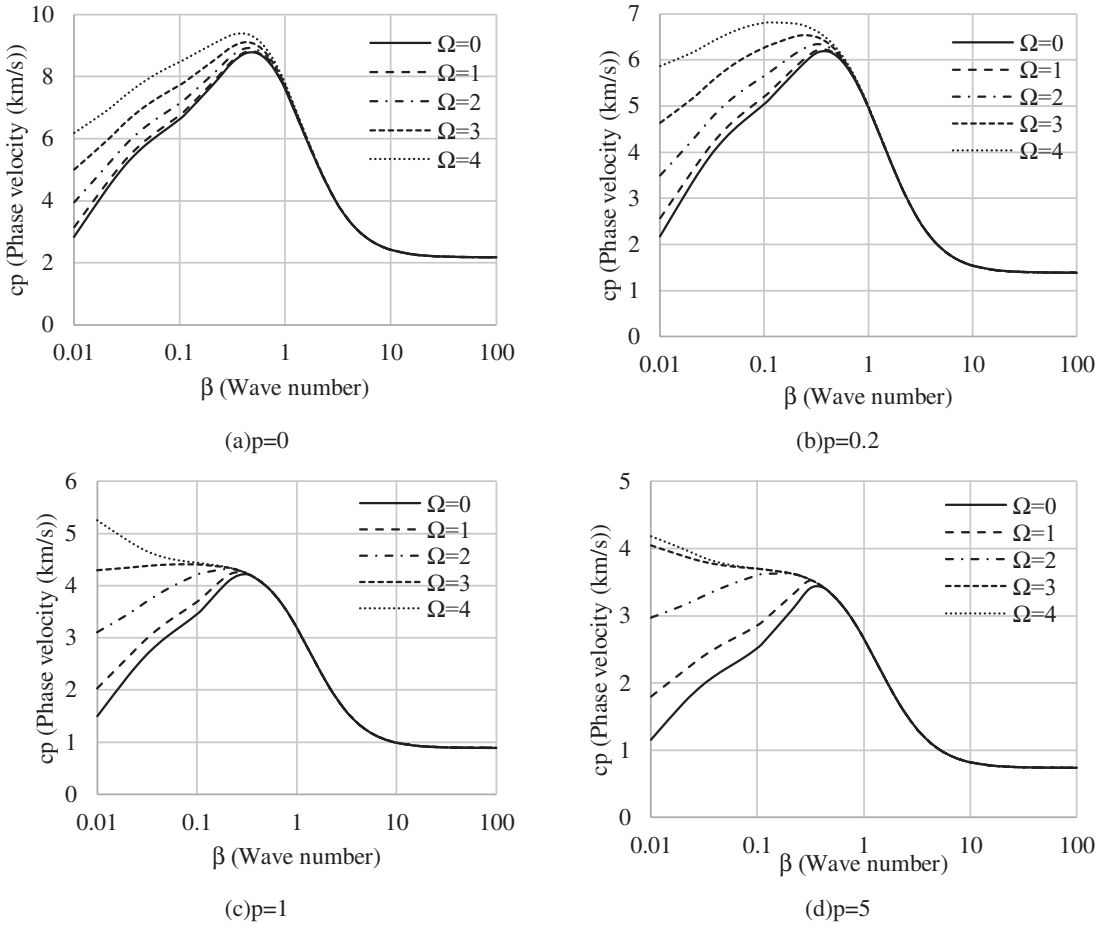

Fig. 2 – Variation of phase velocity of rotating FG nanobeam versus wave number for various angular velocities and gradient indices (NLTR, $\mu = 1$ nm, $\lambda = 0.2$ nm, $\Delta T = 800$).

and 4 for $p = 1$ and 5). But for $\beta \geq 0.9$ (approximately), the phase velocity decreases, then in $\beta \geq 10$ the phase velocity tends to be constant and does not sensibly change with the increase in wave number. In addition, at a constant value of wave number, the phase velocity increases with the increase in angular velocity. However, the diagrams of different angular velocities when $\beta \leq 0.9$ nm are more distinguished and more observable. Thus, the angular velocity of the mentioned nanobeam has no considerable influence on phase velocity at higher values of wave number. Moreover, phase velocity decreases with an increase in gradient index because of the higher portion of metal phase due to an increase in the gradient index.

Fig. 3. indicates the variation of phase velocity of rotating FG nanobeam versus wave number for various length scale parameters ($\lambda = 0.5$ and 1.5) and temperature changes with the constant values of nonlocality parameter ($\mu = 1$ nm) and gradient index ($p = 1$). It is clear that the phase velocity increases due to an increase in wave number. But for $\lambda = 0.5$, after $\beta \geq 0.8$ (approximately), the phase velocity decreases with the increase of wave number. In addition, an increase in the length scale parameter leads to an increase in phase velocity with higher values of wave number. Also, the diagrams of various length scale parameters are distinguished. Moreover, for $\beta \geq 10$ the phase velocity tends to be constant and does not change anymore. Finally, with the increase in temperature change at a constant wave number, the phase velocity decreases. (Fig. 4).

Variation of escape frequency of rotating FG nanobeam versus length scale parameter for various gradient indices with the constant values of nonlocality parameter ($\mu = 1$ nm), temperature change ($\Delta T = 200$) and angular velocity ($\Omega = 2^*10\text{^}9$) for the NLTR temperature distribution is plotted in Fig. 5.

It is observable that, an increase in length scale parameter leads to the increase of escape frequency in a linear way. Also, the escape frequency decreases due to an increase in gradient index.

Variation of escape frequency of rotating FG nanobeam versus angular velocity for various temperature changes and constant values of nonlocality parameter ($\mu = 1$ nm), length scale parameter ($\lambda = 0.2$ nm) and gradient index ($p = 1$) for the NLTR temperature distribution type is reported in Fig. 6. It can be seen that escape frequency decreases due to an increase in temperature change. Also, it is clear that the escape frequency does not sensibly change with the increase in angular velocity.

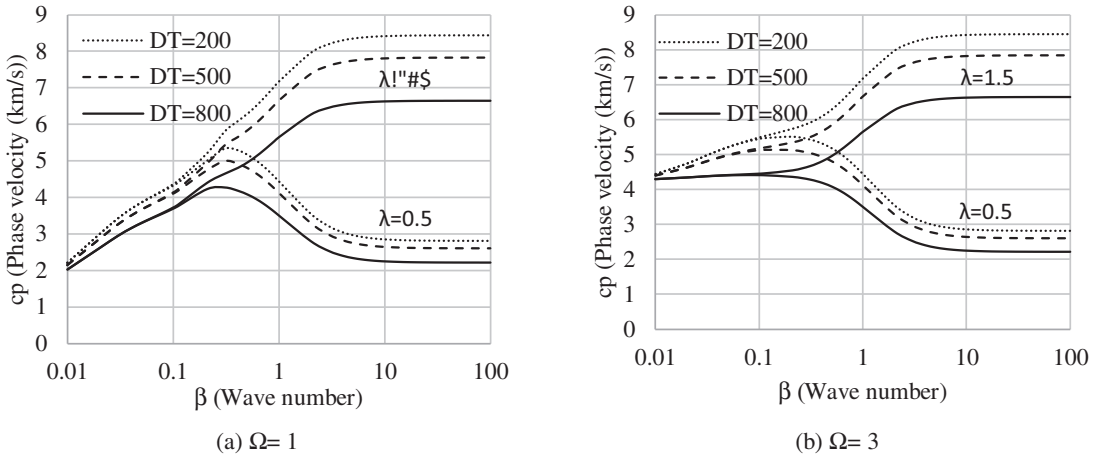

(a) Ω= 1 (b) Ω= 3

Fig. 3 – Variation of phase velocity of rotating FG nanobeam versus wave number for various length scale parameters and temperature changes (NLTR, $\mu = 1$ nm, $p = 1$).

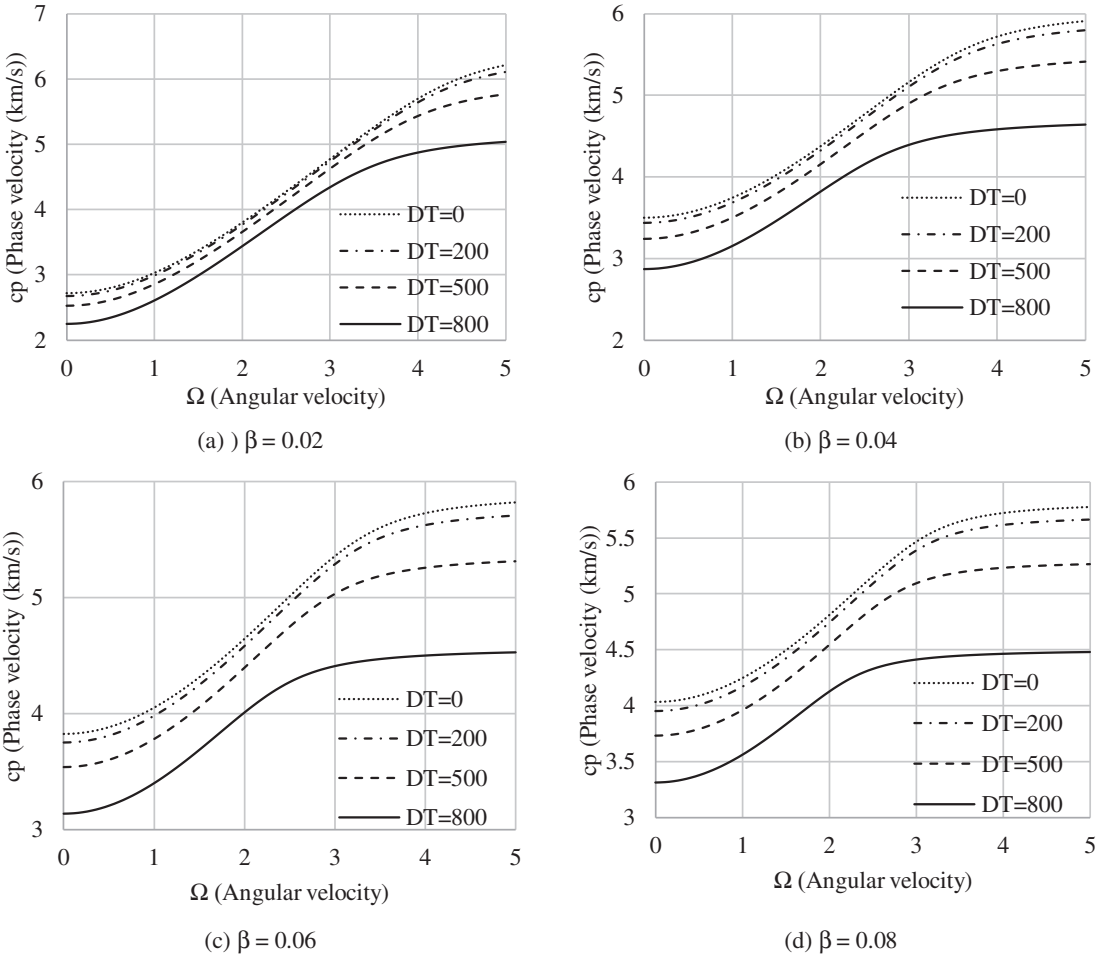

(a)) β = 0.02 (b) β = 0.04

(c) β = 0.06 (d) β = 0.08

Fig. 4 – Variation of phase velocity of rotating FG nanobeam versus angular velocity for various temperature changes (NLTR, $\mu = 1$ nm, $\lambda = 0.5$ nm, $p = 1$).

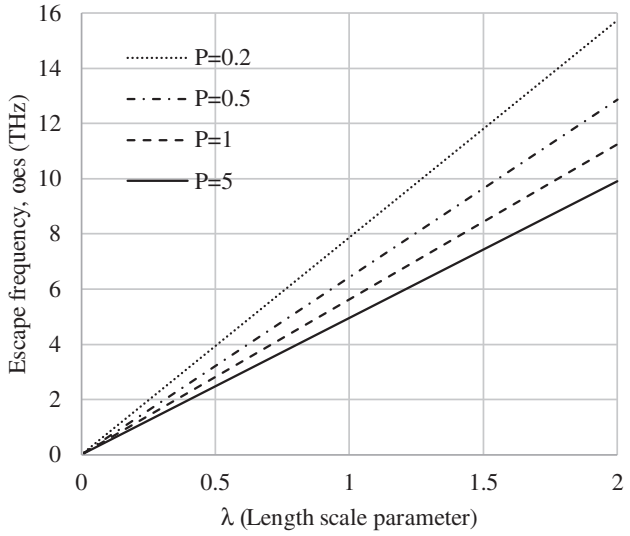

Fig. 5 – Variation of escape frequency of rotating FG nanobeam versus length scale parameter for various gradient indices ($\mu = 1$ nm, $\Delta T = 200$ and $\Omega = 2*10\text{^}9$).

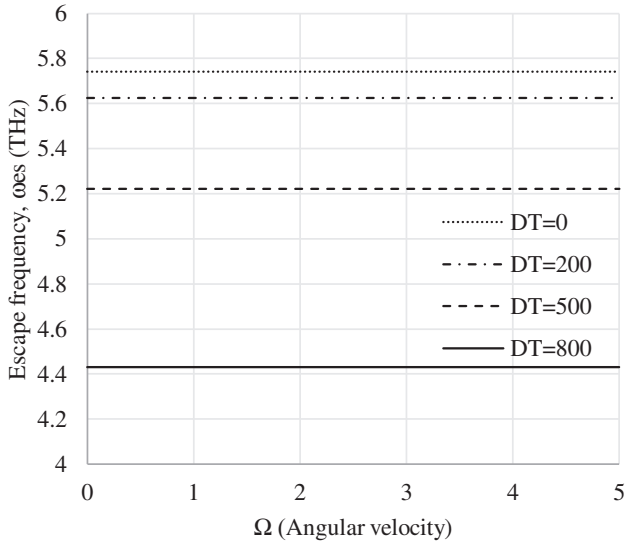

Fig. 6 – Variation of escape frequency of rotating FG nanobeam versus angular velocity for various temperature changes ($\mu = 1$ nm, $\lambda = 0.2$ nm, $p = 1$).

6. Conclusion

In this paper, the wave dispersion characteristics of a rotating thermo-elastic FG nanobeam are explored based on the higher-order refined shear deformable beam theory. The Mori–Tanaka distribution model and nonlocal strain gradient theory are also applied. Through some parametric study, the influences of different parameters such as angular velocity, gradient index, nonlocality parameter, wave number, temperature rise, and temperature distribution on the wave dispersion behavior of the mentioned nanobeam are investigated. It is found that an increase in angular velocity leads to the increase of phase velocity, especially at higher values of angular velocity. However, the increase in angular velocity has no sensible effect on the escape frequency. Also, an increase in wave number causes the increase in phase velocity for lower values of wave number and angular velocity. In addition, phase velocity increases due to an increase in angular velocity, but the diagrams in lower values of wave number are distinguished. Moreover, an increase in length scale causes the increase of escape frequency, but at a constant value of length scale parameter, an increase in the gradient index leads to a decrease in the escape frequency.

REFERENCES

[1] M.A. Eltaher, S.A. Emam, F.F. Mahmoud, Free vibration analysis of functionally graded size-dependent nanobeams, Appl. Math. Comput. 218 (14) (2012) 7406–7420.
[2] F. Ebrahimi, E. Salari, S.A.H. Hosseini, Thermomechanical vibration behavior of FG nanobeams subjected to linear and non-linear temperature distributions, J. Therm. Stresses 38 (12) (2015) 1360–1386.
[3] F. Ebrahimi, E. Salari, Effect of various thermal loadings on buckling and vibrational characteristics of nonlocal temperature-dependent functionally graded nanobeams, Mech. Adv. Mater. Struct. 23 (12) (2016) 1379–1397.
[4] F. Ebrahimi, M.R. Barati, P. Haghi, Nonlocal thermo-elastic wave propagation in temperature-dependent embedded small-scaled nonhomogeneous beams, Eur. Phys. J. Plus 131 (11) (2016) 383.
[5] F. Ebrahimi, M.R. Barati, Thermal environment effects on wave dispersion behavior of inhomogeneous strain gradient nanobeams based on higher order refined beam theory, J. Therm. Stresses 39 (12) (2016) 1560–1571.
[6] M. Ahouel, M.S.A. Houari, E.A. Bedia, A. Tounsi, Size-dependent mechanical behavior of functionally graded trigonometric shear deformable nanobeams including neutral surface position concept, Steel Compos. Struct. 20 (5) (2016) 963–981.
[7] F. Ebrahimi, M.R. Barati, Small-scale effects on hygro-thermo-mechanical vibration of temperature-dependent nonhomogeneous nanoscale beams, Mech. Adv. Mater. Struct. (2016) 1–13.
[8] F. Ebrahimi, M.R. Barati, A unified formulation for dynamic analysis of nonlocal heterogeneous nanobeams in hygro-thermal environment, Appl. Phys. A 122 (9) (2016) 792.
[9] F. Ebrahimi, M.R. Barati, On nonlocal characteristics of curved inhomogeneous Euler–Bernoulli nanobeams under different temperature distributions, Appl. Phys. A 122 (10) (2016) 880.
[10] F. Ebrahimi, M.R. Barati, Wave propagation analysis of quasi-3D FG nanobeams in thermal environment based on nonlocal strain gradient theory, Appl. Phys. A 122 (9) (2016) 843.
[11] F. Ebrahimi, N. Shafiei, Application of Eringen's nonlocal elasticity theory for vibration analysis of rotating functionally graded nanobeams, Smart Struct. Syst. 17 (5) (2016) 837–857.
[12] A.C. Eringen, Linear theory of nonlocal elasticity and dispersion of plane waves, Int. J. Eng. Sci. 10 (5) (1972) 425–435.
[13] A.C. Eringen, On differential equations of nonlocal elasticity and solutions of screw dislocation and surface waves, J. Appl. Phys. 54 (9) (1983) 4703–4710.
[14] A.C. Eringen, Nonlocal Continuum Field Theories, Springer Science & Business Media, 2002.

[15] S. Narendar, S. Gopalakrishnan, Nonlocal scale effects on wave propagation in multi-walled carbon nanotubes, Comput. Mater. Sci. 47 (2) (2009) 526–538.
[16] L. Wang, Wave propagation of fluid-conveying single-walled carbon nanotubes via gradient elasticity theory, Comput. Mater. Sci. 49 (4) (2010) 761–766.
[17] Y. Yang, L. Zhang, C.W. Lim, Wave propagation in double-walled carbon nanotubes on a novel analytically nonlocal Timoshenko-beam model, J. Sound Vibr. 330 (8) (2011) 1704–1717.
[18] S. Narendar, S.S. Gupta, S. Gopalakrishnan, Wave propagation in single-walled carbon nanotube under longitudinal magnetic field using nonlocal Euler–Bernoulli beam theory, Appl. Math. Model. 36 (9) (2012) 4529–4538.
[19] M. Aydogdu, Longitudinal wave propagation in multiwalled carbon nanotubes, Compos. Struct. 107 (2014) 578–584.
[20] S. Filiz, M. Aydogdu, Wave propagation analysis of embedded (coupled) functionally graded nanotubes conveying fluid, Compos. Struct. 132 (2015) 1260–1273.
[21] M.A. Eltaher, M.E. Khater, S.A. Emam, A review on nonlocal elastic models for bending, buckling, vibrations, and wave propagation of nanoscale beams, Appl. Math. Model. 40 (5) (2016) 4109–4128.
[22] D. Srivastava, A phenomenological model of the rotation dynamics of carbon nanotube gears with laser electric fields, Nanotechnology 8 (4) (1997) 186.
[23] S. Zhang, W.K. Liu, R.S. Ruoff, Atomistic simulations of double-walled carbon nanotubes (DWCNTs) as rotational bearings, Nano Lett. 4 (2) (2004) 293–297.
[24] S.C. Pradhan, T. Murmu, Application of nonlocal elasticity and DQM in the flapwise bending vibration of a rotating nanocantilever, Phys. E: Low-Dimens. Syst. Nanostruct. 42 (7) (2010) 1944–1949.
[25] S. Narendar, S. Gopalakrishnan, Nonlocal wave propagation in rotating nanotube, Results Phys. 1 (1) (2011) 17–25.
[26] J. Aranda-Ruiz, J. Loya, J. Fernández-Sáez, Bending vibrations of rotating nonuniform nanocantilevers using the Eringen nonlocal elasticity theory, Compos. Struct. 94 (9) (2012) 2990–3001.
[27] M. Mohammadi, M. Safarabadi, A. Rastgoo, A. Farajpour, Hygro-mechanical vibration analysis of a rotating viscoelastic nanobeam embedded in a visco-Pasternak elastic medium and in a nonlinear thermal environment, Acta Mech. 227 (8) (2016) 2207–2232.
[28] C.W. Lim, Y. Yang, Wave propagation in carbon nanotubes: nonlocal elasticity-induced stiffness and velocity enhancement effects, J. Mech. Mater. Struct. 5 (3) (2010) 459–476.
[29] C.W. Lim, G. Zhang, J.N. Reddy, A higher-order nonlocal elasticity and strain gradient theory and its applications in wave propagation, J. Mech. Phys. Solids 78 (2015) 298–313.
[30] L. Li, X. Li, Y. Hu, Free vibration analysis of nonlocal strain gradient beams made of functionally graded material, Int. J. Eng. Sci. 102 (2016) 77–92.
[31] L. Li, Y. Hu, L. Ling, Flexural wave propagation in small-scaled functionally graded beams via a nonlocal strain gradient theory, Compos. Struct. 133 (2015) 1079–1092.
[32] F. Ebrahimi, M.R. Barati, Flexural wave propagation analysis of embedded S-FGM nanobeams under longitudinal magnetic field based on nonlocal strain gradient theory, Arab. J. Sci. Eng. 42 (2017) 1715, doi:10.1007/s13369-016-2266-4.
[33] S. Narendar, Wave dispersion in functionally graded magneto-electro-elastic nonlocal rod, Aerosp. Sci. Technol. 51 (2016) 42–51.
[34] F. Ebrahimi, M.R. Barati, P. Haghi, Thermal effects on wave propagation characteristics of rotating strain gradient temperature-dependent functionally graded nanoscale beams, J. Therm. Stresses 40 (5) (2017) 535–547.